Theoretical Analysis and Clinical Demonstration of the Effect of Power Pattern Control Using the Annular Phased-Array Hyperthermia System

V. SATHIASEELAN, M. F. ISKANDER, G. C. W. HOWARD, AND N. M. BLEEHEN

Abstract—**The phase and amplitude control of power deposition patterns for the BSD Annular Phased Array (APA) has been theoretically analyzed at a frequency of 60 MHz. Absorbed power patterns in simple circular cross-sectional cylindrical dielectric structures were studied first to compare with published experimental results. Models based on computerized tomography (CT) scans from the pelvic region have been used for predicting the specific absorption rate (SAR) patterns in patients. Significant changes were observed with phase changes of 30° and relative amplitude changes of 20 percent. The theoretical predictions qualitatively agree with the experimental results reported for simple phantoms. It is also shown that these techniques result in a better control of the SAR patterns and thus more effective heating of tumors situated eccentrically within the pelvis, which we have confirmed in clinical treatments.**

I. Introduction

PRELIMINARY REPORTS [1]–[3] indicate that it is possible using the Annular Phased Array (APA)[1] to produce regional pelvic hyperthermia to heat deep-seated tumors to therapeutic temperatures. The critical factors affecting the power deposition patterns of the APA have been studied experimentally by Paul Turner using simple phantoms [4]–[6]. These include the frequency, patient position within the octagonal opening, the relative phase and amplitude of the radiated power from each aperture, size of the water bolus used, and variations in internal tissue structures.

Turner's studies also have shown a strong correlation between external surface electric fields and deep internal field patterns and that to achieve deep heating at the center, it is essential to ensure geometric centering of the patient within the array opening. Four minimally perturbing *E*-Field sensors [4] are provided by the BSD to be placed in axial alignment on the surface of the patient's body within the APA applicator to obtain electric-field balance. This practice of patient positioning is most widely used in the clinic [7] to alter the power deposition pattern. Clinical experience suggests this only provides a limited ability to adjust the balance and location of the heating because of limited space available within the aperture. To obtain better control of absorbed power patterns, the ability to alter the APA power deposition patterns by varying the relative phase and amplitude of the individual aperture radiation has been investigated theoretically.

Experimental investigation is difficult as it is impossible to build a phantom that accounts for anatomical variations within and between patients. However, numerical modeling methods based on exact anatomical data available from computerized tomography (CT) scans have been developed to study the APA [8], [9]. The best approach seems to be to use the theoretical model to calculate the power deposition patterns and then use invasive probes to monitor regions selectively to obtain confirmatory measurements.

This paper will describe the results obtained from such a theoretical study and early clinical data, demonstrating the clinical relevance and usefulness of this technique. Some of the results have been presented previously [10]. Paulsen *et al.* [11] also have shown recently that significant changes can be produced in the power deposition pattern by varying the amplitude and phase of the aperture radiation.

A. APA System

The technical characteristics of the system have been described by Turner [4]. The APA consists of 16 radiating apertures, arranged in two adjacent rings of eight applicators. The operating frequency is in the range 50–100 MHz to obtain deep penetration. The array is powered by four coaxial inputs each activating a quadrant of the array with power fed from a RF generator through a 2-kW amplifier. In normal operation, the applicators are all fed in phase and equal amplitude. The radiation field of the array consists of a cylindrically divergent TEM wave which has its electric field dominantly polarized along the cylindrical axis of the body. The electric field at the center is the sum of the field from each of the applicators, and hence the power deposited is proportional to the square of the number of applicators.

Manuscript received September 18, 1985; revised January 27, 1986.

V. Sathiaseelan is with the Mallinckrodt Institute of Radiology, Washington University Medical Center, St. Louis, MS 63110.

G. C. W. Howard and N. M. Bleehen are with the Medical Research Council Unit and University Department of Clinical Oncology and Radiotherapeutics, MRC Center, Cambridge, CB2 2QH, U.K.

M. F. Iskander is with the Department of Electrical Engineering, University of Utah, Salt Lake City, UT 84112.

IEEE Log Number 8607855.

[1]BSD Medical Corporation, Salt Lake City, UT.

0018-9480/86/0500-0514$01.00 ©1986 IEEE

II. Theoretical Background

The mathematical theory and the moment method solution used in this numerical study has been described in [8]. It has been shown that the integral equation relating the total electric-field E at any point (x, y) inside the body is given by (for $\exp(-jwt)$ time dependence)

$$\boldsymbol{E}(x,y)-\frac{jk_0^2}{4}\cdot\iint_s(\epsilon_{r-1})\boldsymbol{E}(x_0,y_0)\cdot H_0^{(1)}(k_0\rho)\,dx_0\,dy_0=\boldsymbol{E}^I(x,y) \quad (1)$$

where $k_0=2\pi/\lambda_0$, λ_0 is the free space wavelength, $H_0^{(1)}(k_0\rho)$ is the Hankel function of zero order, and ρ is given by

$$\rho=\sqrt{(x-x_0)^2+(y-y_0)^2}. \quad (2)$$

The coordinate system used is shown in Fig. 1(a) and the integration is over the cross section of the two-dimensional body.

$\boldsymbol{E}^I$ is the total incident field from the aperture sources and is given by

$$\boldsymbol{E}^I=\hat{z}\sum_{i=1}^{8}E_i(x,y) \quad (3)$$

where E_i is the incident field from each of the eight aperture sources. The incident electric field is assumed to be polarized along the z direction.

The incident field at any point is given in terms of the aperture field distribution $E_z(x_0,0)$ by [12]

$$E_i(x,y)=-\frac{j}{2}\frac{\partial}{\partial n}\cdot\int E_z(x_0,0)H_0^{(1)}\left[k\left\{(x-x_0)^2+y_0^2\right\}^{1/2}\right]dx_0 \quad (4)$$

where the integration is over the intersection of the aperture with the plane $y=0$.

The numerical solution of (1) then involves dividing the cross section into N small cells, assuming the field to be constant in each, and employing the point-matching technique to discretize the equation to [12]

$$\boldsymbol{E}_m-\frac{jk_0^2}{4}\sum_{n=1}^{N}(\epsilon_n-1)\boldsymbol{E}_n\iint_{\text{cell}}H_0^{(1)}(k_0\rho_m)\,dx_0\,dy_0=\boldsymbol{E}_m^I,\quad m=1,2,3,\cdots N \quad (5)$$

where ϵ_n and $\boldsymbol{E}_n$ are, respectively, the complex permittivity and the unknown total electric field in the cell n. Equation (5) is then a simple system of linear equations with the values of E being the unknown coefficients to be determined. The integration in (5), over the cell cross section, was done in closed form assuming a circular cell of equivalent area, as described in [13].

The absorbed power density or specific absorption rate (SAR) in the tissue for each cell is given by

$$\text{SAR}=\frac{1}{2}\frac{\sigma}{\rho}|\boldsymbol{E}|^2\ \text{W/kg} \quad (6)$$

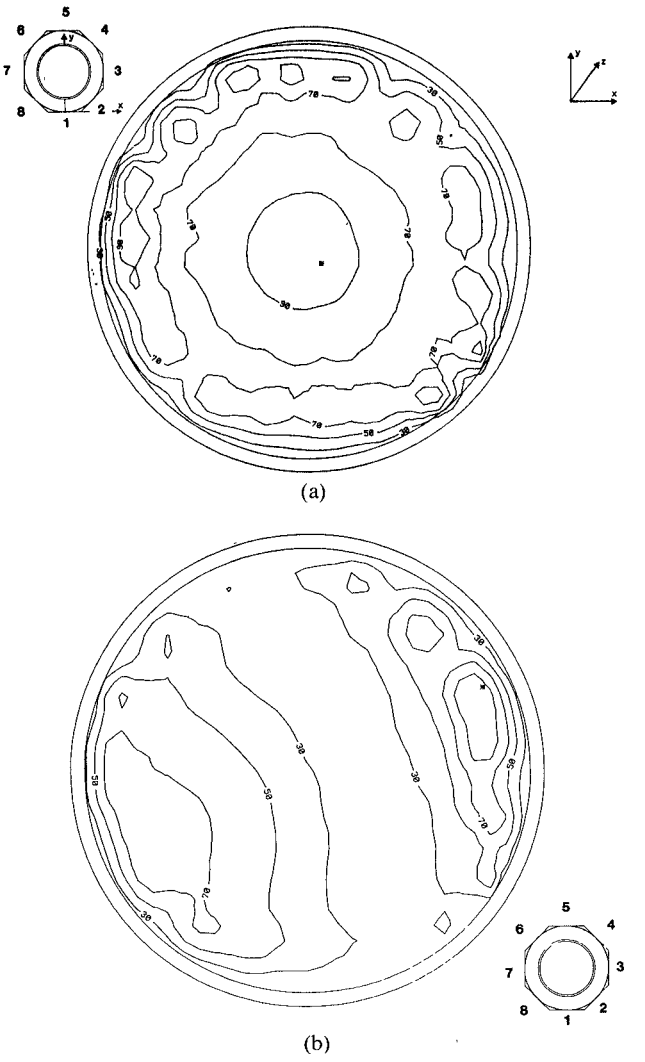

Fig. 1. Phase control on absorbed power for cylindrical model. Normalized percent (30,50,70,90) SAR contours: (a) Equiphase excitation on all apertures, (b) 65°-phase lag on apertures 1,6,7,8.

where σ is the conductivity (S/m) and ρ is the density (kg/m) of the tissue in the cell.

A. Aperture Field Distribution

The field distribution on each of the eight apertures has been modeled as a half wavelength cosine function whose peak value is located at the center.

$$E_a=E_0\cos\left(\frac{\pi x}{A}\right)\qquad \text{for}-\frac{A}{2}\leq x\leq\frac{A}{2} \quad (7)$$

where A is the length of the segment and x is the distance along the segment.

Relative phase shift was introduced by adding the component $\exp(j\phi)$ to each of the aperture field source terms, where ϕ is either zero or the required phase shift.

III. Numerical Results and Discussion

A. Cylindrical Model

A circular cylindrical structure placed centrally in the APA was studied first to compare with Turner's experimental results [6]. This homogeneous model also provides a

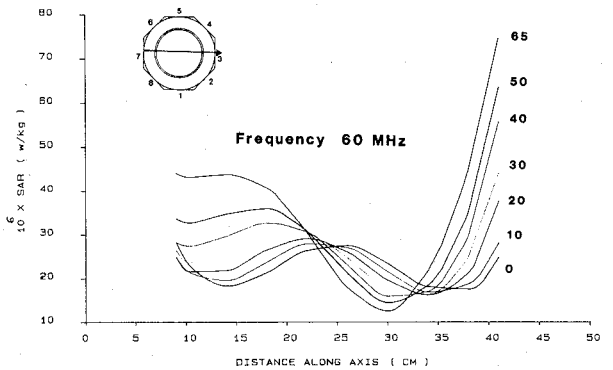

Fig. 2. Computer SAR scan for the cylindrical model along a diameter parallel to the x axis.

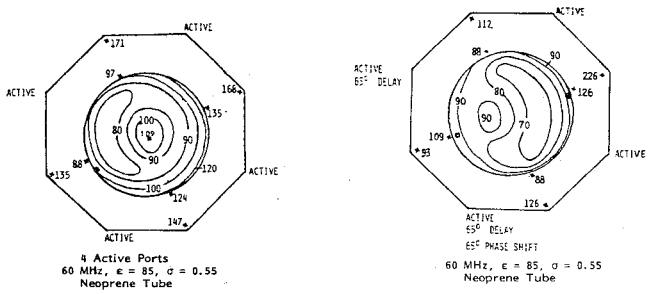

Fig. 3. Experimental results for cylindrical phantom ([15] with permission from IEEE).

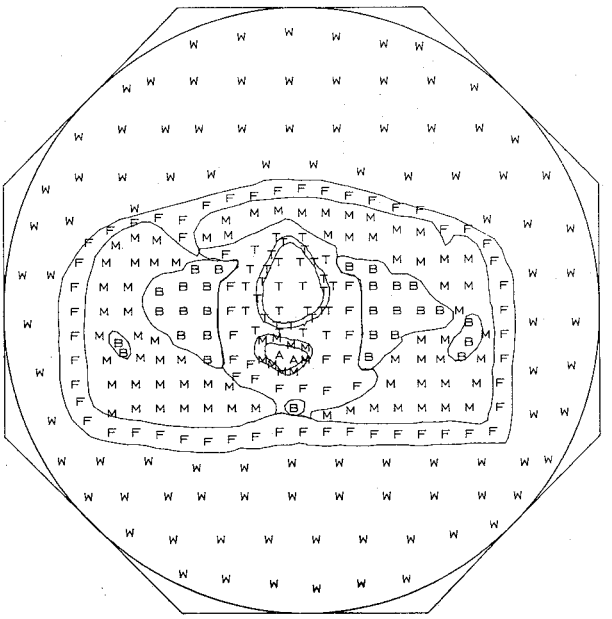

Fig. 4. Representative cross section of the human pelvis located inside APA configuration. Letters designate different tissues as given in Table I.

good check for the validity of the numerical method. The resulting SAR pattern, across the cross section for synchronous excitation, must be symmetrical about the z axis because of the symmetrical nature of the model. The inner diameter of the cylinder is 32 cm with a wall thickness of 1 cm. The wall is assumed to be made of neoprene rubber with dielectric properties of $\epsilon = 10.0$ and $\sigma = 0.02$ (S/m) at 60 MHz. The cyclinder is filled with saline solution ($\epsilon = 85.0$ and $\sigma = 0.55$ S/m) and the bolus contains distilled deionized water ($\epsilon = 79.0$ and $\sigma = 0.0$ S/m). These are values reported by Turner [6]. The cross-sectional area was divided into 184 cells.

The SAR patterns obtained for synchronous excitation and 65°-phase lag on apertures 1,6,7,8 are shown in Fig. 1(a),(b), respectively. Since the apertures are excited in pairs, this is the most feasible excitation method to produce relative phase difference between apertures without physically modifying the APA. The SAR contours shown are the 30-, 50-, 70-, and 90-percent values of the maximum SAR calculated within the cylindrical structure. The location of this maximum value is indicated on the figures by an asterisk (*).

A symmetrical SAR pattern with the central maximum heating zone is obtained for synchronous excitation as shown in Fig. 1(a). This is expected as the radiated electromagnetic waves from the apertures overlap and interact to create a standing wave pattern with an equal phase reinforcement at the center (can be considered as a focal point) of the APA opening.

The existence of the standing wave is demonstrated in Fig. 2 where calculated SAR scans along a diameter of the cylinder (parallel to the X axis) for phase lags in steps of 10° are shown. A significant shift in the central maximum heating zone towards the phase-lag apertures (1,6,7,8) can be seen for phase lags of greater than 30°. As the central heating zone shifts towards the phase-lag apertures, a region of high-power deposition is also produced at the opposite end. This is due to the high-field strengths at the edge of the standing wave patterns, which exist for synchronous excitation in the bolus bag region outside the cylindrical phantom, now moving correspondingly into the phantom. The shifting of the central heating zone can be thought to be due to the displacement towards the delayed phase apertures of the point of equal phase reinforcement of the interacting waves.

These predicted pattern shifts qualitatively agree with the experimental observations of Turner shown in Fig. 3. The shift of the maximum central heating zone and the presence of the high-power deposition region diagonally opposite the phase-lag apertures can be seen clearly.

B. Pelvic Model

The pelvic model shown in Fig. 4 was divided into 306 cells. The cell centers are denoted by the respective tissue they represent. The different tissue types used and their dielectric properties and tissue densities are given in Table I. A region around and including the bladder is considered to be a tumor. Currently available dielectric data based mainly on in-vitro measurements, for example [14], indicate the tumor properties to be similar to high water content tissues, e.g., muscle tissue, in the frequency range of interest. Hence, in the present study, the tumor dielectric properties have been taken to be the same as muscle tissue.

The normalized percent SAR contours (30, 50, 70, and 90 percent) for synchronous and phase delay 65° are shown in Fig. 5(a), (b). The shifting of the pattern is quite evident.

The maximum power deposition occurs in the region designated as tumor for synchronous excitation. The body was slightly off-centered, hence a region of high-power

TABLE I
PROPERTIES OF TISSUE USED IN THE COMPUTER PROGRAM

name	at 60 MHZ ϵ	σ (S/m)	ρ (Kg/m)
Muscle (M)	85.0	0.55	1.02×10^3
Tumour (T)	85.0	0.55	1.02×10^3
Fat (F)	10.0	0.02	0.9×10^3
Bone (B)	10.0	0.02	1.79×10^3
Distilled water (W)	79.0	0.0	1.0×10^3
Air (A)	1.0	0.0	

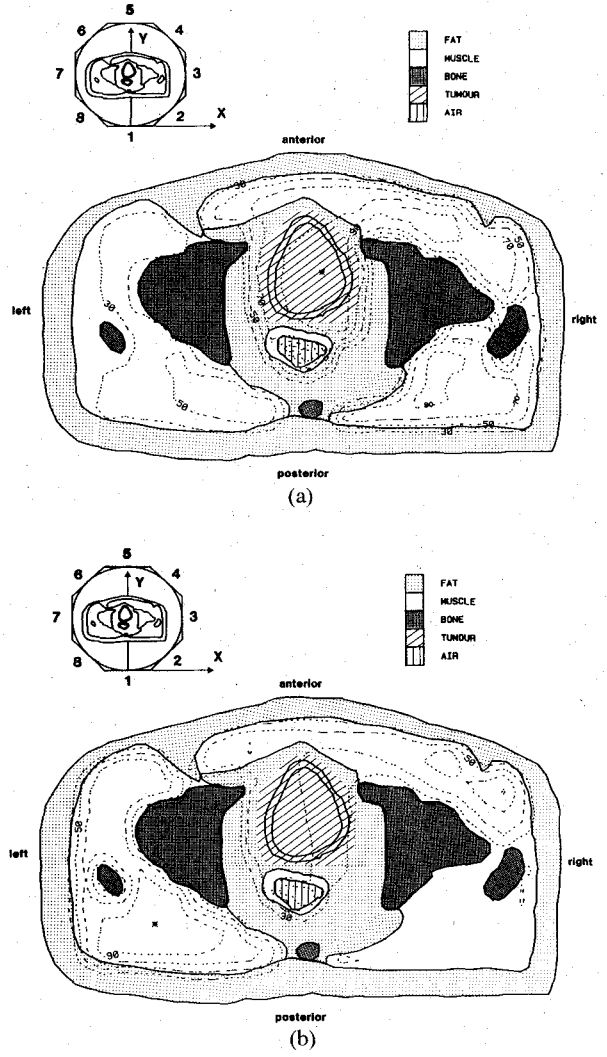

Fig. 5. Phase control on absorbed power for pelvic model. Normalized percent (30,50,70,90) SAR contours: (a) Equiphase excitation on all apertures, (b) 65°-phase lag on apertures 1,6,7,8.

deposition can be observed near the right posterior region of the pelvis. This may explain our experience that during some treatments, patients have complained of pain in this area. This may be an optimistic situation as the tumor was modeled electrically equivalent to muscle tissue (having

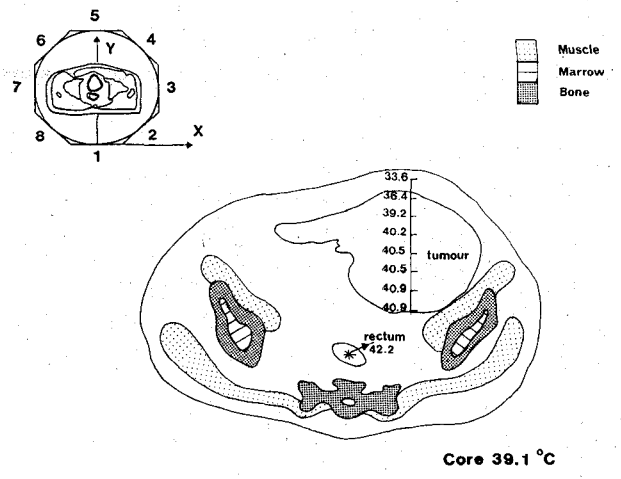

Fig. 6. Measured temperature distribution in a pelvic tumor obtained at 1-cm intervals during treatment of a patient in the APA with standard set up of equal phase excitation on all apertures.

relatively high conductivity in relation to other surrounding tissue, mainly fat). Power absorption is primarily dictated by the conductivity (6), since the E-field distribution does not vary a great deal within the structure. Obviously lower electrical conductivities will result in less absorbed power.

Similar observations have been made by Paulsen *et al.* [9], where they have found that the calculated electric fields generated by the APA for three different body cross sections showed striking similarities despite their many anatomical differences. A maximum usually occurred near the center of the patient, but the ratio of E_{max}/E_{min} was less then two throughout the body cross section. Our study too, showed similar variations.

To demonstrate the potential usefulness of this technique, the temperature distribution obtained during the treatment of a large tumor situated eccentrically in the pelvis is shown in Fig. 6. Temperatures at 1-cm intervals were obtained by manually scanning a temperature probe across the center of the tumor. Another temperature probe was placed in the rectum of the patient. The heating was performed by positioning the patient centrally in the APA and as expected from the theoretical calculations, the temperature measured in the centrally placed rectal probe is much higher than that achieved in the tumor. On the other hand, if we had been able to shift the power distribution as shown in Fig. 7, using 40-percent amplitude reduction on apertures (1,6,7,8) and 65°-phase lag on apertures (2,3,4,5), we should have produced a more effective heating of the tumor. Obviously it is not possible to correlate directly the absorbed power patterns with the expected temperature distribution because the heat dissipation due to blood flow and thermal conduction would markedly modify the temperature pattern. However, it is generally accepted that in large tumors, the central area is necrotic with low blood flow. Hence, the peak temperature increases can be expected to occur in areas where maximum power is deposited provided it is in the center of the tumor.

It must also be stated that the CT-scan used in the model is not from the patient in whom the temperature distribution was obtained. But this example was used to illustrate the usefulness of the power shifting capability. In

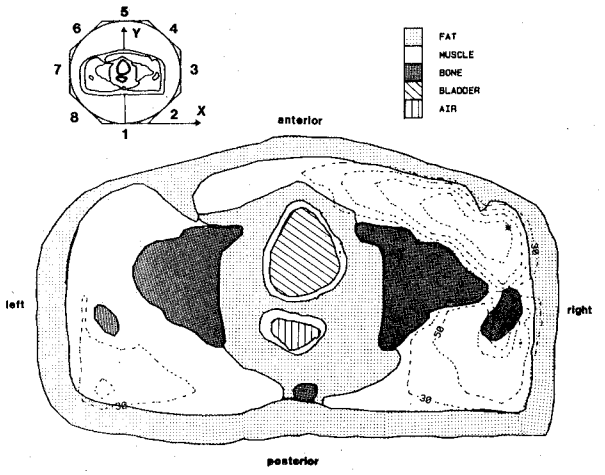

Fig. 7. Computed normalized SAR contours for 65°-phase lag on apertures 2,3,4,5 and 40-percent amplitude reduction on apertures 1,6,7,8 for a representative patient volume.

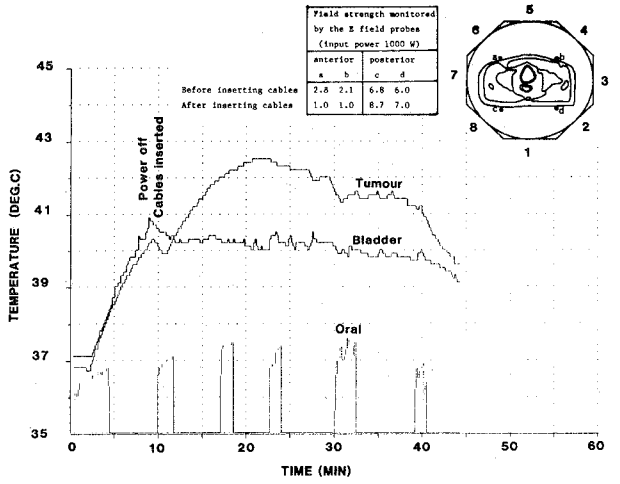

Fig. 8. Temperature profiles obtained during treatment demonstrating the effect of phase control.

practice, a relative phase difference can be created for the four quadrants by altering the length of the input cable with respect to that of the other quadrants by inserting additional cable or using line stretchers. High-power variable attenuators have to be used to control the power in each segment of the APA. It will be quite difficult to perform these controls routinely in the clinic during treatments with the present version of the APA. However, it is possible with suitable modifications to excite the APA directly from a multichannel amplifier [15] where the controls can be performed by using a microcomputer.

The technique of phase control by varying the lengths of feed cables has now been used in the treatment of several patients. Our early experience seems to confirm the predicted change in SAR patterns with phase control and an example is shown in Fig. 8. The patient had a recurrent rectal carcinoma situated posteriorly in the pelvis in the presacral hollow. Intratumor temperatures were monitored along a cannula inserted through a perineal sinus. The bladder temperatures were monitored through a urinary catheter. Oral temperature was monitored intermittently. The patient was positioned to obtain maximum heating posteriorly as can be seen from the higher posteriorly placed E-field probe readings in Fig. 8. Initially both the posteriorly situated tumor, and anteriorly situated bladder increase in temperature equally, with the bladder being marginally hotter after 8-min treatment. The power was then switched off and cables of lengths 63.8 cm were added to the feed cables exciting aperture pairs (8,1) and (2,3), to produce a phase lag of 65° to try and shift the SAR pattern posteriorly. The shift in the SAR patterns was confirmed by the higher values recorded by the posteriorly placed E-field probes (c, d) compared to the anteriorly placed probes (a, b). A reduction of more than 100 percent was observed for the anterior probes. Following this, the tumor heated preferentially resulting in a temperature differential of 2.5°C. This resulted in a much more satisfactory treatment than would otherwise have been possible.

IV. Conclusions

The results of the theoretical study indicate that it is possible to shift the absorbed power patterns by varying the phase and/or amplitude of the excitation of the apertures. The theoretical results for the simple cylindrical model agree qualitatively with the experimental results reported by Turner. A significant shift in the central maximum heating zone toward the phase-lag apertures were observed with phase changes of greater than 30°. The patterns shifted towards higher levels of excitation for relative amplitude changes of greater than 20 percent. Using a model based on individual patients CT scan, the predicted power pattern shift with phase control has been confirmed in the clinic. Early clinical testing seems to indicate this is a feasible and useful technique.

Acknowledgment

The authors gratefully acknowledge the assistance of S. Mounsey of the MRC Cancer Trials Office, Cambridge, England, in all the computer programming aspects of this work. They thank S. J. Thomas (Medical Physics Dept., Addenbrookes Hospital, Cambridge, England) for the help in obtaining digitized patient data from the CT scans and appreciate very much the useful discussions with Dr. G. A. King (Dept. of Radiology, SUNY Upstate Medical Center, Syracuse, NY). They also thank the reviewer's constructive comments and for providing [11].

References

[1] M. D. Sapozink, F. A. Gibbs, J. W. Thomson, J. R. Eltringham, and J. R. Stewart, "A comparison of deep regional hyperthermia from an annular array and a concentric coil in the same patients," *Int. J. Rad. Oncol. Biol. Phys.*, vol. 11, no. 1, pp. 179–190, Jan. 1985.

[2] B. Emami, C. Perez, G. Nussbaum, and L. Leybovich, "Regional hyperthermia in treatment of recurrent deep-seated tumors: Preliminary report," in *Hyperthermic Oncology 1984*, vol. 1, J. Overgaard, Ed. London: Taylor and Francis, pp. 605–608, 1984.

[3] G. C. W. Howard, V. Sathiaseelan, G. A. King and N. M. Bleehen, "Early experience with the BSD clinical hyperthermia system," *Strahlentherapie*, vol. 161, no. 9, p. 536, 1985.

[4] P. F. Turner, "Regional hyperthermia with an annular phased array," *IEEE Trans. Biomed. Eng.*, vol. BME-31, no. 1, pp. 106–114, Jan. 1984.

[5] P. F. Turner, "Hyperthermia and inhomogeneous tissue effects using an annular phased array," *IEEE Trans. Microwave Theory Tech.*, vol. MTT-32, no. 8, pp. 874–882, Aug. 1984.

[6] P. G. Turner, "Electromagnetic hyperthermia devices and methods," M.S. thesis, Dep. Elec. Eng., Univ. Utah, Salt Lake City, June 1983.
[7] F. A. Gibbs, M. D. Sapozink, K. S. Gates, and J. R. Stewart "Regional hyperthermia with an annular phased array in the experimental treatment of cancer: Report of work in progress with a technical emphasis," *IEEE Trans. Biomed. Eng.*, vol. BME-31, no. 1, pp. 115–119, Jan. 1984.
[8] M. F. Iskander, P. F. Turner, J. B. DuBow, and J. Kao, "Two-dimensional technique to calculate the EM-power deposition patterns in the human body," *J. Microwave Power*, vol. 17, no. 3, 1982.
[9] K. D. Paulsen, J. W. Strohbehn, and D. R. Lynch, "Theoretical thermal dosimetry produced by an annular phased-array-type system in CT-based patient model," *Radiat. Res.*, vol. 100, pp. 536–552, 1984.
[10] V. Sathiaseelan, M. F. Iskander, G. C. W. Howard, S. Crocker, and N. M. Bleehen, "Theoretically predicted effect of phase and amplitude variations on the electromagnetic power-deposition patterns for the annular phased-array hyperthermia system," *Strahlentherapie*, vol. 161, no. 9, p. 549, 1985.
[11] K. D. Paulsen, J. W. Strohbehn, and D. R. Lynch, "Theoretical analysis of the benefits of amplitude and phase control for an annular phased-array hyperthermia system for cancer therapy," in *Proc. 11th Northeast Bioeng. Conf.*, W. S. Kuklinski and W. J. Ohley, Eds., Worcester Polytechnic Inst., Mar. 14–15, 1985, pp. 74–77.
[12] M. F. Iskander, R. Maini, C. H. Durney, and D. G. Bragg, "A microwave method for measuring changes in lung water content: Numerical simulation," *IEEE Trans. Biomed. Eng.*, vol. BME-28, no. 12, pp. 797–804, Dec. 1981.
[13] M. F. Iskander, "Electromagnetic power deposition in biological models: Numerical calculations and phantom measurements," in *Physical Aspects of Hyperthermia*, G. H. Nussbaum, Ed. New York: Amer. Inst. Phys., 1982, pp. 471–479.
[14] R. Peloso, D. T. Tuma, and R. K. Jain, "Dielectric properties of solid tumors during normothermia and hyperthermia," *IEEE Trans. Biomed. Eng.*, vol. BME-31, no. 11, pp. 725–728, Nov 1984.
[15] V. Sathiaseelan, G. C. W. Howard, N. M. Bleehen, I. Har-Kedar, and D. M. Cattermole, "A microcomputer-controlled multiapplicator microwave heating system," in *Hyperthermic Oncology 1984*, vol. 1, J. Overgaard, Ed. London: Taylor and Francis, pp. 695–698, 1984.

✠

V. Sathiaseelan, photograph and biography unavailable at the time of publication.

✠

M. F. Iskander, photograph and biography unavailable at the time of publication.

✠

G. C. W. Howard, photograph and biography unavailable at the time of publication.

✠

N. M. Bleehen, photograph and biography unavailable at the time of publication.